Performance Analysis of LoRaWAN in Industrial Scenarios

Davide Magrin, *Member, IEEE*, Martina Capuzzo, *Student Member, IEEE*, Andrea Zanella, *Senior Member, IEEE*, Lorenzo Vangelista, *Senior Member, IEEE*, and Michele Zorzi, *Fellow, IEEE*

***Abstract*—In this article, we evaluate the performance of a LoRaWAN network in industrial scenarios where different Industrial Internet of Things (IIoT) end nodes communicate to a central controller in order to provide monitoring and sensing information to optimize the efficiency of industrial processes and reduce costs. In particular, we consider confirmed and unconfirmed traffic, multigateway deployments, the usage of different classes of devices, and a nonstandard channel plan. Furthermore, we analyze the higher-layer impact of different models of LoRa PHY layer with industrial channel models. We show that, with proper configuration, LoRaWAN is able to serve IIoT sensing applications with a packet success rate over 90%, providing at the same time limited communication delays.**

***Index Terms*—Industrial communication, interchannel interference, LoRaWAN, ns-3, simulation, telecommunication network reliability, wireless sensor networks.**

I. Introduction

ONE of the key concepts in Industry 4.0 is that of IIoT, with the aim of connecting production machinery to information systems and business processes, in order to optimize the industrial operations and quickly reconfigure the production chains to respond to demand changes [1]. The industrial scenarios differ from other Internet of Things (IoT) environments in three specific aspects: The industrial wireless channel, the traffic patterns, and the Quality of Service (QoS) requirements. Indeed, when compared to a typical IoT smart city scenario, a smart factory scenario presents higher interference and stronger signal attenuation. Furthermore, packets are generated more frequently and need to be delivered with higher reliability and controlled latency.

The most popular low power wide area network (LPWAN) technologies are LoRaWAN, Sigfox, and NB-IoT. These solutions are typically employed in IoT scenarios such as smart cities, but their robustness to channel impairments and high energy efficiency also appeal to the monitoring use cases of IIoT.

Differently from other IoT technologies such as Sigfox, LoRaWAN allows for the creation of a proprietary network, giving full control of the infrastructure and of the network configuration. In general, a tighter control of the network makes it possible to improve the communication latency and reliability compared to public networks, which normally target a large number of diverse use cases.

Despite the growing body of literature in this field, a number of key questions remain unanswered.

1) Which channel and interference models are appropriate to accurately simulate a LoRaWAN deployment in an industrial scenario? How does this choice affect higher-layer performance?
2) How many infrastructure nodes (gateways) do we need to support IIoT applications?
3) What kind of influence do deployment decisions such as channel plan and class of LoRaWAN devices have on the network performance?
4) To improve reliability, is it more convenient to use confirmed traffic or to blindly replicate uplink transmissions?
5) Is LoRaWAN compliant with key communication service requirements for asset and process monitoring in IIoT applications?

The aim of this article is to address such questions and provide insights on the potential and limits of legacy LoRaWAN technologies in the IIoT domain. To this end, we will present a set of detailed simulation results that focus on the most significant high-level performance metrics for industrial applications, using the realistic, measurement-based channel model [2].

In particular, we introduce some specific physical layer (PHY) aspects that have not been studied in the literature so far, such as the presence of out-of-band (OOB) emissions. Moreover, we analyze the medium access control layer (MAC) features affecting the system level performance that are most relevant

Manuscript received February 29, 2020; revised August 6, 2020, October 20, 2020, and November 20, 2020; accepted November 30, 2020. Date of publication December 15, 2020; date of current version June 16, 2021. This work was supported in part by the MIUR (Italian Ministry for Education and Research) under the initiative "Departments of Excellence" (Law 232/2016). Paper no. TII-20-1074. *(Corresponding author: Davide Magrin.)*

Davide Magrin, Martina Capuzzo, and Michele Zorzi are with the Department of Information Engineering (DEI), University of Padova, 35131 Padova, Italy (e-mail: magrinda@dei.unipd.it; capuzzom@dei.unipd.it; zorzi@dei.unipd.it).

Andrea Zanella and Lorenzo Vangelista are with the Department of Information Engineering (DEI), University of Padova, 35131 Padova, Italy and also with Human Inspired Technology (HIT) Center, University of Padova, 35131 Padova, Italy (e-mail: zanella@dei.unipd.it; lorenzo.vangelista@unipd.it).

Color versions of one or more figures in this article are available at https://doi.org/10.1109/TII.2020.3044942.

Digital Object Identifier 10.1109/TII.2020.3044942

for industrial scenarios, such as transmission reliability and latency.

The rest of this article is organized as follows. Section II introduces the main features of the LoRa and LoRaWAN technologies, while Section III reviews the literature that deals with this topic. Our simulation setup is presented in Section IV, while in Section V we analyze the network performance by considering the questions presented above, and discuss the corresponding results. Finally, Section VI concludes this article.

II. Technology Overview

In this section, we present the main aspects of LoRaWAN and of the underlying LoRa modulation.

A. LoRa Modulation

The LoRa modulation, patented by Semtech, is based on the chirp spread spectrum (CSS) technique. The robustness of the modulation can be adjusted by tuning the spreading factor (SF) parameter, which takes integer values from 7 to 12. The SF is directly connected to the data rate: Higher SF allow the transmitted signal to be more robust and to achieve longer coverage range, but at the price of a lower data rate and, thus, longer transmission times. One strength of the LoRa modulation is that signals modulated with different SF are almost orthogonal: Two signals can be simultaneously decoded even if they overlap in time and frequency, provided that they satisfy some mild conditions on the relative received powers as outlined in [3]. Similarly, when multiple signals modulated with the same SF overlap at the receiver, one signal can be correctly demodulated if its power is at least ρ dB higher than the sum of the powers of the interferers (capture effect). The co-channel rejection threshold ρ is specified in LoRa chip datasheets [4], [5], and can be as large as 25 dB for SF 12, as estimated in [3].

B. LoRaWAN Specifications

The LoRaWAN specifications have been developed by the LoRa Alliance [6], and include the description of the MAC protocol layer. LoRaWAN networks have a star-of-stars topology with three kinds of devices.

1) End device (ED) are peripheral nodes, usually sensors or actuators, that communicate using the LoRa modulation.
2) Gateway (GW) are relay nodes that collect messages coming from the ED through the LoRa interface, and forward them to the network server (NS) using a reliable IP connection, and vice-versa;
3) The NS acts as a central network controller that manages the communication with the ED through the GW.

When the ED transmit, the LoRa packets are collected by all the GW in their coverage range and forwarded to the NS, which discards duplicates and chooses the best GW for the return transmissions to the ED. It is worth noting that the GW do not support full-duplex transmission: To send a downlink (DL) packet (from the NS to an ED), they have to interrupt any ongoing uplink (UL) reception.

TABLE I
Available LoRaWAN Channels

Frequency [MHz]	Use	Duty Cycle	Maximum ERP
868.1	UL/DL	1%, shared	14 dBm
868.3	UL/DL	1%, shared	14 dBm
868.5	UL/DL	1%, shared	14 dBm
869.525	DL	10%, dedicated	27 dBm

The LoRaWAN specifications define three classes of ED, which differ in terms of energy saving capabilities and reception availability. Class A devices stay in sleep mode most of the time in order to minimize the energy consumption, transmit a packet whenever required by the application layer, and open only two reception windows after each transmission. Class B devices periodically open reception windows, following the scheduling information provided in periodic beacon messages sent by the GW. Class C devices usually are powered by the main electric grid and consequently can keep the reception window always open to get DL messages, when not transmitting.

Moreover, the specifications define two types of messages: Confirmed and unconfirmed. For the first case, an acknowledgment (ACK) packet is expected by the ED, in either of the two reception windows opened after the transmission. ED have m transmission opportunities: If the ACK is not received,[1] the ED can retransmit the packet up to $m-1$ times. Unconfirmed messages, instead, do not require any ACK.

LoRaWAN operates in the unlicensed industrial, scientific, and medical (ISM) frequency bands. The relevant regulations define frequency bands, power, and duty cycle (DC) restrictions to be applied. In Table I, we report the default values for the European region as recommended by the LoRaWAN specifications; although the use of additional channels on other subbands is permitted, in this article we focus on the minimum frequency set mandated by the specifications. Here, LoRaWAN [6] defines the use of three 125-kHz wide channels, centered at 868.1, 868.3, 868.5 MHz, which are shared between UL and DL transmissions, and must collectively respect a 1% DC constraint [7]. As per the specification [6], a fourth 125-kHz channel centered at 869.525 MHz is used for DL communication only, and is subject to a DC constraint of 10% [7]. Note that also the maximum transmission power differs, being 14 dBm in the shared channels and 27 dBm in the DL-only channel [7].

In this article, we assume that ED access the channel according to a pure ALOHA scheme and, hence, are subject to the duty cycle limits that, in Europe, are specified by the ETSI recommendations [8]. Note that, by using a combination of listen before talk (LBT) and adaptive frequency agility (AFA) access schemes, the DC constraint can be relaxed to 2.8% for any 200-kHz spectrum [8]. A comparison between ALOHA and LBT+AFA access schemes in LPWAN is presented, e.g., in [9], [10], and [11], where the authors generally conclude that

[1] For both Class A and Class C devices, a retransmission is triggered if no reply is received within 2 s after the end of the transmission plus the time needed to detect a LoRa signal. This guarantees that the ACK delay performance of Class C devices is, at worst, equal to that of Class A devices within a time interval that extends to the end of the second receive window.

LBT+AFA can indeed bring a (limited) performance gain over ALOHA, in particular in green-field scenarios (i.e., when all nodes use the same access method), even though [9] shows that ALOHA turns out to be more robust than LBT+AFA in mixed scenarios. In this article, we choose to focus on the ALOHA mode only, which is the chosen access scheme for LoRa in Europe.

The LoRaWAN specifications also allow for the use of a single 250-kHz channel with SF 7 for the transmission of UL packets in the European region. The wider bandwidth makes it possible to transmit the same message in half the time, reducing the collision probability. Once the bandwidth is defined, there is a one-to-one correspondence between SF and data rate (DR). According to the LoRaWAN specifications, the rates indicated with DR0 to DR5 correspond to SF 12 to 7, respectively, with 125-kHz channel, while DR6 corresponds to SF 7 with a 250-kHz channel. In this article, we assume that all devices will use the same data rate, either SF 7 on a 125-kHz channel (DR 5) or SF 7 with a 250-kHz channel (DR 6) for UL communication. When devices employ SF 7 with a 125-kHz bandwidth, three channels at 868.1, 868.3, and 868.5 MHz are available for UL transmissions. Instead, when SF 7 is used with a 250-kHz bandwidth, all UL transmissions will use the same frequency at 868.3 MHz, foregoing the benefit of frequency orthogonality within the considered network deployment.

For Class A devices, the standard requires the first receive window (RX1) to be opened in the same frequency channel and with the same SF used for the UL communication. The RX2, instead, is always opened on the dedicated 869.525-MHz channel and with SF 12, in order to maximize the robustness of the communication. These standard settings can be changed by using appropriate MAC commands sent by the NS. However, for RX1, only SF higher than that used in UL can be set, since the ED is assumed to use the lowest SF that allows the GW to receive its signal. If a lower SF were used in DL, the message could arrive at the ED with a power level below the sensitivity, preventing its correct reception. Class C devices, instead, when not transmitting or receiving in RX1, are always listening in RX2 using the default parameters.

III. State of the Art

Even though different works present applications of wireless communications in industrial scenarios (e.g., [12]–[14]) it is a common opinion that, because of the multiple and contrasting requirements of IIoT applications, there is no unique solution that fits all the use cases [15], [16]. The work in [17] compares from the technical point of view different LPWAN technologies for the machine-to-machine (M2M) scenario, and concludes that LoRaWAN is suitable for both smart city applications and industrial use cases where a small volume of data is required, but in this article no evaluation results are provided.

The LoRaWAN performance is, instead, evaluated in [18] and [19], where the authors identify confirmed traffic as potentially damaging for the system performance if transmission and reception parameters are not properly configured. For instance, repetitions can decrease the network throughput and scalability, making devices unnecessarily consume more energy. In this case, the introduction of confirmed traffic, which had the goal of increasing the communication reliability, ends up being counterproductive. A study on how the network parameters could be set to reduce these negative effects is proposed in [20], where extensive ns-3 [21] simulations analyze the impact of many network configurations on the system performance when using both confirmed and unconfirmed traffic; however, only a smart city scenario with a single GW is considered. The authors in [22], instead, propose time and antenna diversity to increase LoRa performance. Repetition coding in particular is proven to be an effective choice, provided that SF and the number of replicas are always chosen in order to avoid flooding the network with useless repetitions. Improving the underlying network infrastructure is another approach that can be used to achieve a higher reliability. The authors in [23], for example, simulate in ns-3 a multi-GW LoRaWAN deployment with confirmed traffic in a smart city scenario. As expected, the availability of a multi-GW infrastructure brings several benefits to the network. In addition to the possibility of employing lower SF in a dense deployment, a higher number of GW makes it possible to share the load of downlink traffic, overcoming DC limitations and increasing the number of reply messages sent in RX1, which prevents sensor nodes from opening both receive windows.

The aforementioned works target an urban scenario, since the LoRaWAN technology was first proposed as a solution for IoT in large areas and open-air environments. Measurements of LoRa coverage range and signal-to-noise ratio (SNR) within an industrial plant are presented in [24]. The authors find that a single GW is sufficient to cover an area of 34 000 m^2, and simulations based on the measured values estimate a network capacity of about 6000 nodes. The performance in terms of robustness to the noise and packet loss at the PHY layer is presented in [25], which analyzes the LoRa technology in an industrial setting, where machinery is deployed. The work proposed in [26] explores LoRa performance in different indoor settings, also providing a characterization of the channel. In [27], the authors present the results of an experimental campaign assessing the LoRaWAN performance in an indoor deployment with single-GW and only unconfirmed UL traffic, exploring different metrics, such as throughput, coverage, and power consumption. Energy efficiency of LoRaWAN devices in an industrial scenario and the tradeoff between transmission periodicity and battery replacement costs are also investigated in [28]. In [29], the authors compare the performance of LoRaWAN and IEEE 802.15.4 for an industrial scenario with unconfirmed traffic, proving the effectiveness of LoRaWAN.

Recent works have considered possible improvements of the LoRaWAN technology to address industrial requirements, such as latency and reliability, with new techniques. In [30], the authors show that a scheme combining time division multiple access (TDMA) and frequency hopping is compatible with soft real-time applications, and that proper time, frequency, and SF planning makes it possible to obtain the same performance of well-established technologies for industrial applications, such as WirelessHART and ISA100.11a, achieving a network capacity of 6000 ED transmitting a packet every minute. Similarly,

in [31], the authors ameliorate the network performance by using cyclically scheduled super-frames split in intervals reserved for different types of communications. The authors in [32] consider the integration of a LoRaWAN deployment with 4G/5G networks for the IIoT, with a LoRa GW acting as a base station connected to the cellular network, and performing all the required LTE signaling, control, and security procedures.

In this article, instead, we investigate the performance of a LoRaWAN deployment, as defined in the specifications, and show how it performs in industrial scenarios when using multigateway deployments, confirmed traffic, Class C devices, and alternative channel plans. Different from previous works that suggest deeper changes to the medium access logic of the LoRaWAN protocol, all the solutions explored in this article can be implemented by simple configurations that can be applied also to already widely available devices, and can thus be more easily deployed and maintained.

IV. Scenario

In this section, we describe in detail the scenario and the models we considered in our simulations. We use the ns-3 `lorawan` module, also employed in [20], which makes it possible to consider the effect of confirmed DL traffic in the network. The simulator has been further extended to support the various settings discussed in the following sections.

A. Industrial Scenario

We consider a LoRaWAN deployment in an industrial plant and assume that nodes are uniformly spread in a rectangular area with size 200 × 200 m^2, similar to the case considered in [24]. We assume ED are wireless sensor nodes for process and asset monitoring, e.g., collecting measurements of temperature, pressure, or flow rates. We simulate a network composed of 300 ED, i.e., one device every ∼133 m^2, that transmit periodic updates with a period $T \in \{30, 300\,000\}$ s, thus getting an application-layer offered traffic load of $\lambda \in \{0.001, 10\}$ pkt/s. Note that this deployment is quite different from a typical smart city use case [33], where a GW serves thousands of devices over an area with a radius of several kilometers. We simulate networks with only unconfirmed or only confirmed traffic. In the latter case, the number m of maximum transmissions per packet is typically set to 1 or 4. Similarly, we consider the possibility of repeating the transmission of unconfirmed packets k times, as a measure to increase robustness of UL communication. This simple repetition coding increases the reliability and does not occupy the GW with DL ACK transmissions, which have been proved to be a bottleneck when the goal is to maximize the delivery of UL data [20], [23]. Application-layer packet size is set to 20 bytes for UL messages, while DL packets are assumed to carry only the ACK contained in the LoRaWAN header. When a single GW is simulated, it is placed on the middle point of one of the edges of the rectangle containing the ED, while uniform random allocation within the limits of the rectangle is chosen for scenarios with multiple GW. Given the short distance between the ED and the GW, all ED are configured to employ SF 7. Similarly, RX2 SF is set to 7 to maximize the data rate. This choice is motivated by some preliminary tests which showed that, for the simulated values of the offered traffic λ, this is the most efficient solution.

TABLE II
Path Loss Coefficients for Industrial Propagation Channel

Reference	Scenario	d_0 [m]	L_0 [dB]	η	σ [dB]
[35]	Assembly Room	2	25	1.72	3.8
	Electronics Room	2	26	1.96	2.29
	Mechanical Room	2	26	1.79	5.07
[2]	LOS	15	57.67	2.25	5.65
	NLOS, lightClutter	15	64.42	1.94	4.97
	NLOS, heavyClutter	15	69.73	2.16	5.16

B. Channel Model

In this article, we assume that LoRaWAN works in the 863–870-MHz band, employing the minimum set of channels required by the specifications (see Table I). The industrial wireless channel is particularly complex, and models need to take into account the presence of obstacles, signal reflections, delays, and intermittent noise caused by machines. In this article we account for three main effects typically present in this environment. 1) Path loss and large-scale effects, which consider the signal attenuation caused by the distance between transmitter and receiver and by the presence of obstacles, 2) small-scale effects, which consider reflections of the signal in the surrounding environment, and 3) shot noise.

The total loss due to large-scale effects, $L(d)$, can be expressed in dB as the sum of path loss and shadowing

$$L(d)_{dB} = PL(d)_{dB} + \chi_{dB}. \tag{1}$$

The term χ_{dB} is usually modeled as a zero-mean Gaussian random variable with standard deviation σ, as defined in Table II. For the path loss component, $PL(d)$, the loss is commonly computed according to the distance from the transmitter using a single-slope propagation loss model [2], [34]:

$$PL(d)_{dB} = \begin{cases} L_0 + 10\eta \log_{10}\left(\frac{d}{d_0}\right), & d > d_0 \\ L_0, & d \le d_0 \end{cases}. \tag{2}$$

The estimation of the path loss coefficients in industrial scenarios has been the subject of many studies, such as [2], [34], and [35]. In this article, we compare the system performance in multiple propagation scenarios, for which the path loss and shadowing terms have different values. In [35] test transmissions are performed from a height of 15 m, with the receiver placed near the ground, and the path loss coefficients are estimated for three rooms in a plant, which differ for the density of machines, the position of objects in the space, and the material they are made of. We refer to the three scenarios modeled in this article as *assembly room*, *electronics room*, and *mechanical room*. In [2], the receiver is placed at a height of 6 m, while transmitting sensors are placed 2-m above the ground level. This work defines three additional propagation scenarios: Line-of-sight (LOS) when a direct path exists between transmitter and receiver, and light/heavy clutter when the height of the obstacles which obstruct the path are comparable to/much higher than the height of the sensor, respectively. The parameters

for the selected models are listed in Table II; in Section V-A we compare the behavior of the LoRaWAN system when using these models with the outcome of experimental measurements obtained from the literature [24], and motivate the choice of a model that will be used throughout the remainder of the article.

Small-scale effects account for the reflections of the transmitted signal in the propagation environment. These variations in the signal strength are modeled through a Nakagami-m distribution [36]. The value of the coefficient for the Nakagami-m distribution m_N is computed according to the channel model we implement. The channel model provided in [2] estimates temporal fading coefficients with log-normal distribution with mean 12.3 dB and standard deviation 5.4 dB. In the other cases, we used $m_N = 1.41$, as estimated in [37].[2]

Finally, we take into account the fact that an industrial environment may contain machinery creating additional background noise. In [38] and [39] the authors characterize the shot noise in an industrial setting, estimating the cumulative distribution function (CDF) of the peak amplitude with respect to the noise floor, of the pulse duration and of the interval between consecutive pulses. The duration of the pulses turns out to be between tens of nanoseconds and a few microseconds, while the pulse spacing ranges from 100 ns to 204 μs. In our simulations, with a LoRa packet lasting tens of milliseconds, the introduction of an interference source with these features would lead to a high increase of the computational cost, which would be unnecessary given the interference model we consider (see Section IV-C). Although PHY level simulations showed that shot noise has no tangible impact on the demodulation performance of a single LoRa symbol, aggregate effects might still be present when an entire LoRa transmission is taken into consideration. Thus, in this article we take a conservative approach, and account for the effect of shot noise by increasing the additional average noise power within a typical LoRa transmission, by a value of 3 dB based on the statistical description of the noise provided in [38].

C. Interference Models

The literature features several approaches to model the interference in LoRaWAN networks. According to [3], the interference among the spreading factors can be modeled through a "co-channel rejection matrix," where each element $e_{i,j}$ represents the power gap in dB that a signal transmitted with SF i must have to survive an interferer using SF j. As in [40], we assume that the interleaver will spread out the interferer's energy on the entire received packet. Thus, if two received signals overlap for a certain time T_I, the interference power will be multiplied by the ratio T_I/T, where T is the duration of the desired signal, before being compared to the threshold. In the following, we will call this approach *Simple*, as it only employs this threshold matrix to decide whether a packet is lost because of interference.

A different solution is proposed in [23] and [29]. Here, the received signal is divided into chunks with constant signal-to-interference-plus-noise ratio (SINR). The error rate of each chunk is computed by multiplying the length of the chunk by the bit error rate (BER) corresponding to the SINR and SF of the signal, and the packet success probability is derived as the product of each individual chunk's success probability. Additionally, the authors in [29] leverage the two aforementioned approaches by combining signal-to-interference ratio (SIR) and SNR in a measure called "equivalent SIR," for which the BER for different SF are computed. In the following, this approach will be referred to as *Spectrum*, as it employs the `spectrum` framework provided by ns-3.

Finally, in this article we also consider the effect of OOB emissions. OOB is an undesired effect in radio systems that consists in the emission of power in frequency bands adjacent to the nominal transmission band. In particular, OOB emissions for LoRa are described and measured in [41]. Although the OOB power level is much lower than in the nominal band, the OOB emissions contribute to increasing the amount of interference, and this could be relevant in particular situations, e.g., when two devices are in close proximity, or when a strong signal coming from an ED in one channel interferes with a weak signal coming from a different ED operating in a neighboring channel. The impact of OOB can be exacerbated by the so-called carrier frequency offset (CFO), i.e., the offset that affects low-cost frequency oscillators. The CFO can shift the carrier frequency up to 30 kHz. GW, which employ more expensive circuitry, are designed to be robust to these impairments and can still correctly demodulate transmissions whose frequency error falls within a range of $\pm$30 kHz [42]. However, such an overlap may increase the effect of OOB. We hence introduce the *SpectrumOOB*, where out-of-band emissions contribute to the interference suffered by the desired signals. In this model, we add side lobes to transmissions in the frequency domain, possibly spilling into adjacent channels. Similarly to the Spectrum interference model, the decrease in performance caused by this additional interference is then modeled through the "equivalent SIR" method employed in [29].

D. Performance Metrics

For the network evaluation, we define the following metrics, with the aim of capturing the communication performance, and assessing the capabilities and effectiveness of a LoRaWAN deployment for sensing purposes in an industrial plant.

1) The *uplink packet delivery ratio* measures the fraction of UL packets successfully delivered to the GW over those generated by the applications at the ED. A success corresponds to the correct delivery of *at least* one copy of a UL packet. According to whether the UL traffic is carried by confirmed or unconfirmed packets, this metric is named *confirmed uplink PDR (CU)* or *unconfirmed uplink PDR (UU)*, respectively.
2) The *delay* of a UL transmission is defined as the time between the packet generation and the moment it is successfully received by at least one GW and becomes then available to the NS.
3) The *confirmed packet success rate (CPSR)* is the probability that both the UL packet and the corresponding ACK are correctly received by the NS and by the ED, respectively. This metric is meaningful only for confirmed

[2]We recall that the coefficient m_N for the Nakagami propagation model can be obtained from the K-factor of Rician channel models as $m_N = (K^2 + 2K + 1)/(2K + 1)$.

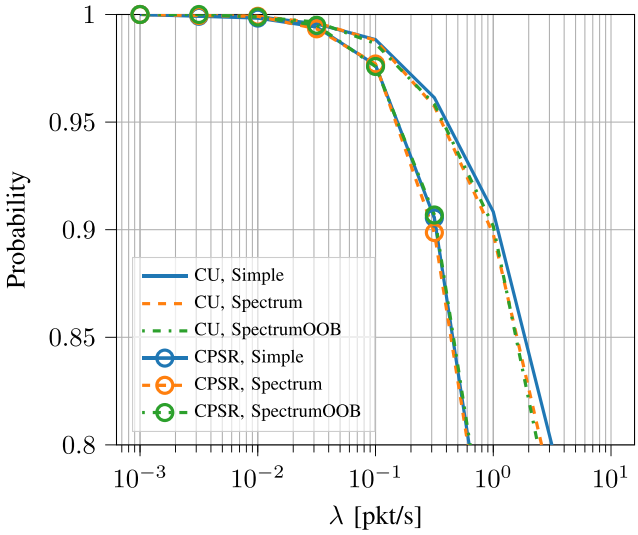

Fig. 1. Comparison of different interference models in terms of CU and CPSR, in a network served by a single GW.

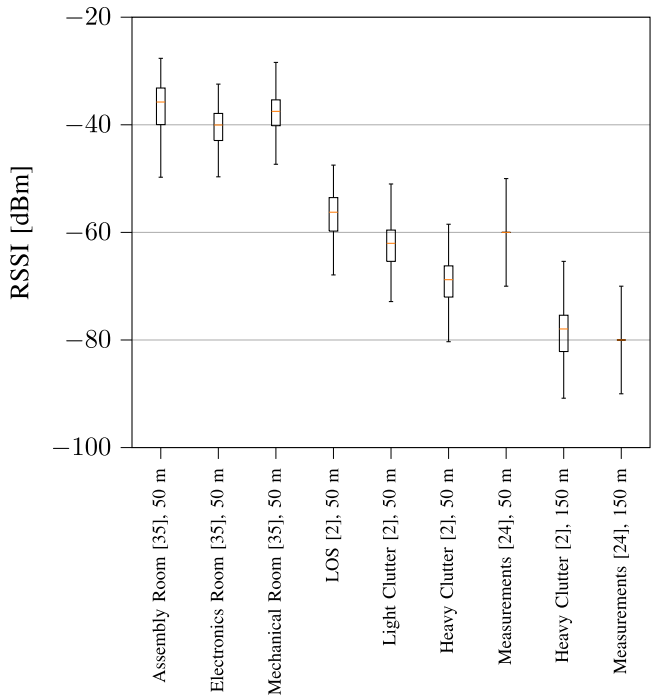

Fig. 2. Received signal strength indicator (RSSI) computed from different propagation models and experimental measurements.

traffic, and represents the capability of the system to communicate to the ED, i.e., transmitting short control messages in response to UL updates or queries, or assessing the reliability of the connection, avoiding further retransmissions.

4) Finally, the *ACK delay* is defined as the time from the generation of a confirmed UL packet to the successful reception of the corresponding ACK at the ED.

V. Results

This section describes the simulation results and analyzes the tradeoffs involved in the design of a LoRaWAN solution for industrial applications. Given the large number of error and propagation models available in the literature, a first batch of simulation results explores their impact on the network performance in the considered scenario. Based on these considerations, an error and a propagation model are chosen for the rest of the simulations to investigate the higher-layer effects of the density of GW deployment, the class of device and the chosen channel plan.

A. Comparison of Error and Propagation Models

Fig. 1 shows the simulation outcomes when the Simple, Spectrum, and SpectrumOOB interference models are used to evaluate the CU and CPSR performance. When confirmed traffic and retransmissions are considered, the different interference models yield quite similar performance. This suggests that the additional interference due to OOB emissions has limited impact on the MAC performance in the considered scenario. It should be noted that a slight increase in the SINR experienced by devices was observed in simulation, especially for higher values of λ. In these cases, however, the MAC level performance is largely dominated by direct collisions between transmissions overlapping in time and frequency. Similarly, the overall effect of OOB emissions at the network level when frequency shifts due to imprecise oscillators were included in the simulator was found to be negligible. These results motivate us to neglect the effects of OOB and imperfect oscillators, and to use the Spectrum interference model in the following analysis. This model is preferred to the SpectrumOOB model for its lower computational complexity, while maintaining the effects of propagation environments that the Simple model ignores.

Fig. 2 shows the distribution of the simulated RSSI according to the different propagation models listed in Table II. The figure shows that the models described in [2] and [35] provide quite different outputs. When we compare these results with the outcomes measured experimentally in [24], also shown in Fig. 2 for distances of 50 and 150 m, it becomes apparent that the models in [2] provide better estimates of the experimental RSSI measurements. In particular, the samples collected in [24] at 50 m, which were almost always in LOS conditions, are closely represented by the LOS model, while measurements at over 150 m, in non line-of-sight (NLOS) conditions, can be matched using the heavy clutter propagation model. Based on this, the results presented in the remainder of this article have been obtained by considering a piecewise propagation loss model, in which the LOS parameters are used when the transmitter–receiver distance is lower than 100 m, and the heavy clutter model is used for distances over 100 m.

We also remark that, in addition to RSSI measurements, the authors in [24] provide SNR values. When comparing such values with those computed in our simulations, we found that the latter were consistently 20-dB above the experimental ones. The reason is that the SNR provided by LoRa chipsets saturates to around 12 dB for RSSI values significantly above sensitivity, irrespective of the actual RSSI value [43].

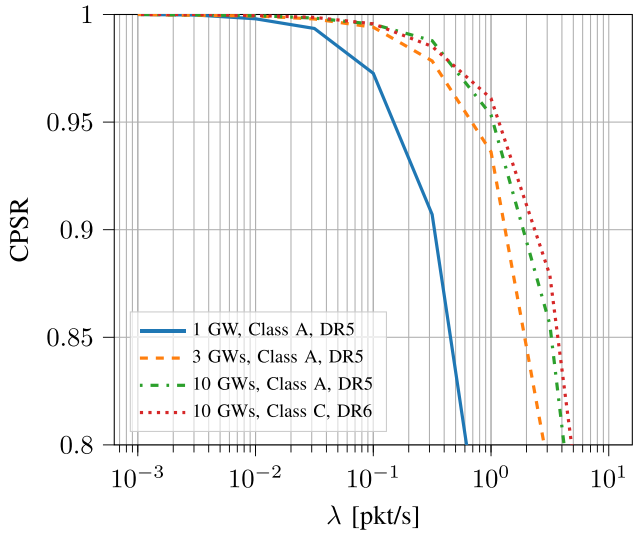

Fig. 3. Effect of gateway deployment density in terms of CPSR for $m = 1$.

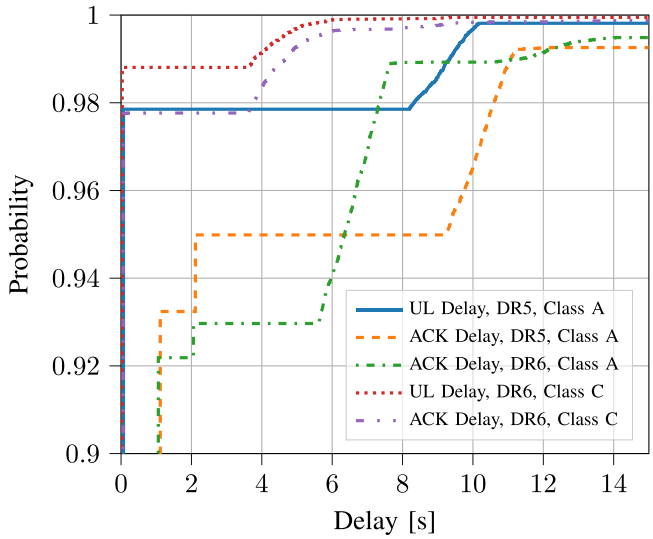

Fig. 4. Empirical CDF for different delay metrics and network configurations.

B. Increasing the Number of Deployed GW

In this section, we evaluate the network performance for different GW densities. The GW are uniformly placed inside the same area of the ED. Having multiple GW improves the network performance by increasing the DL transmission capacity and the diversity in the wireless channels. The former advantage alleviates the effect of the duty cycle limitations that impose silent periods to the GW: With multiple GW, the probability that at least one is available to transmit a DL packet increases.

Fig. 3 shows that a larger number of GW positively affects the ACK delivery rate for confirmed traffic (CPSR) even with $m = 1$. Although we have not reported the plots for space constraints, we also ran simulations for $m = 4$ and high traffic load, i.e., $\lambda = 10$ pck/s in this specific scenario, obtaining a CPSR of 99.7% with 10 GW, and above 99.99% with 20 GW. Very similar gains were observed for the UU and CU metrics.

Fig. 4 shows the empirical CDF of UL and ACK delays for confirmed traffic in a network served by 10 GW, with $m = 4$ and $\lambda = 1$ pck/s. Despite the fact that, with these settings, the network is able to eventually deliver over 99.9% of its UL MAC-layer packets and 99% of its DL messages, the plot highlights the large delay due to duty cycle limitations and the receive window design for Class A devices, for which the minimum possible ACK delay is a little over 1 s. For a fraction of devices, the first receive window remains empty, and therefore they have to wait for a DL message in the second receive window. If this reception fails, the next retransmission opportunity is available well over 9 s after the generation of the first UL message, due to duty cycle restrictions. In addition to this forced pause, in which the ED is in sleep mode, the standard requires an additional back-off, uniformly distributed between 1 and 3 s before the retransmission attempt, further increasing the delay experienced by the ED, which corresponds to the slope of the curve in Fig. 4. These results confirm that increasing the number of GW can be a very effective strategy to increase the probability of correct message delivery in both the UL and DL directions, as predicted. Furthermore, coupling this setting with an increase of the retransmissions is shown here to be a viable strategy to improve reliability in industrial scenarios.

Although increasing the GW density is a very simple and straightforward way to boost the reliability of the transmissions and to reduce the packet delay, placing GW uniformly over the coverage area in industrial deployments might not always be possible, and companies might be forced to place GW at the edge of the facility, as done in [24]. This configuration was actually proven to be beneficial because of the increased channel diversity in [44].

C. Class C Devices and DR6

In this section, we describe the simulation results obtained when Class C ED and DR6 are employed in the network. Employing a bandwidth of 250-kHz halves the duration of the transmissions, yielding a very small gain in both the UL and ACK delay metrics with respect to the default configuration. However, this shorter time on air also cuts roughly by half the waiting times before retries caused by duty cycle restrictions, allowing the devices to retransmit about 5 s after their initial attempt, instead of around 9 s when DR5 is employed. This advantage comes at the cost of additional interference, because all the ED contend for the same frequency. Therefore, the application of this single-channel plan may not always be beneficial for all the devices. Indeed, in Fig. 4, the CDF of ACK delay for DR6-Class A setting is lower than for a DR5-Class A setting up to a delay of approximately 6.2 s. The combination of Class C and DR6, instead, provides very significant gains for both the delay metrics, reducing the minimum possible ACK delay from 1 s to the bare transmission time of a pair of UL and DL packets, which is in the order of a hundred milliseconds. This gain requires the LoRaWAN sensor node constantly attached to a main power source, or at least accepting a drastic reduction of battery lifetime. Nonetheless, this result proves that satisfactory delays both in the UL and in the DL are possible for over 99% of the devices in LoRaWAN with the right combination of network

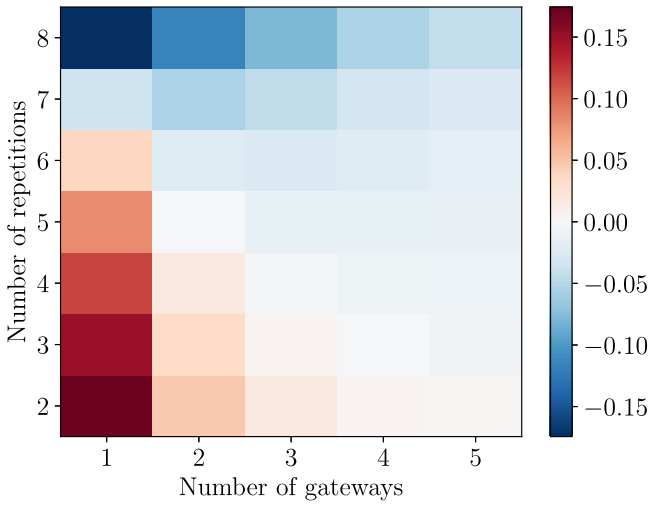

Fig. 5. Improvement in UU performance when using repetitions instead of confirmed traffic.

settings, for an offered traffic of $\lambda = 1$ pck/s. Finally, the CPSR with DR6-Class C setting is more effective than doubling the number of GW in the network, as can be seen from Fig. 3.

D. Confirmed Traffic and Repetitions for Reliability

In this section, we assess the effect on the UU metric of employing k "blind" repetitions of each UL packet in a network using unconfirmed traffic, as opposed to employing up to m transmissions per packet when using confirmed traffic. In the first case, we assume that the application always transmits each packet k times. In the second scenario, instead, retransmissions are performed by the ED only if no ACK is received. For these simulations we consider Class A devices with three channels to transmit. Furthermore, we set $\lambda = 10$ pck/s to better highlight the differences between the two approaches.

In both cases, we can observe that increasing the number of GW has a positive effect on the UU performance, albeit with diminishing returns. With confirmed traffic, a sufficient number of GW is necessary to have a stable network: If the NS is not able to promptly respond to every ACK request, UL traffic can quickly increase because of retransmissions, further worsening the situation. The number of repetitions k, instead, is a critical parameter for the unconfirmed traffic case. In general, we can see that the blind repetition of UL messages yields better performance than relying on confirmed transmissions because the former can leverage the time diversity in the repetitions, without suffering from the GW unavailability due to DL transmissions.

Fig. 5 shows the difference between the unconfirmed and the confirmed solutions, for different values of $k = m$ and of the number of GW serving the network. Especially for underprovisioned networks, the unconfirmed scenario provides significant gains with respect to the confirmed scenario, provided that the number of retransmissions is well dimensioned. It should also be noted that, for a sufficiently large number of GW, the difference between the two approaches becomes negligible, as the GW can serve all devices, also when the traffic is increased because of repetitions.

E. Evaluation of Communication Service Metrics

In this section, we evaluate the performance reached by LoRaWAN with respect to the service requirements for process and asset monitoring as defined in [45]. In particular, we consider sensors generating periodic measurements of a continuous value, such as temperature or pressure. In this case, the maximum allowed end-to-end latency is 100 ms, and the period between consecutive data transmissions is 60 s with uniformly distributed deviations of $\pm 25\%$ around the target value. When a packet delivery is not completed within the specified end-to-end latency, the system is said to experience a failure. Two metrics are considered.

1) *Communication Service Reliability*: Ability of the communication system to perform as required for a given time interval [45]. In our case, the reliability is quantified with the mean time between failures.
2) *Communication Service Availability*: Fraction of time during which the communication service operates without failures over the total amount of time the system is expected to deliver the service, in percentage.

Due to the heavy duty cycle limitation and the slow bit rate, only a single transmission can fit within the end-to-end latency requirement described above, considering that LoRa transmissions typically last in the order of tens of milliseconds. In this case, since SF orthogonality is not leveraged (only DR 5 and DR 6 are used, in order to limit the delay and channel occupation), and since the LoRaWAN MAC protocol targets applications with sporadic traffic, only a few tens of devices can be supported with a communication reliability of 10 min, and an availability over 90%. These results are obtained with the best configuration we identified, i.e., Class C devices and 10 GW with 3 frequency channels.

If the application requirements are more lenient, with an end-to-end latency of 60 s (thus allowing up to $m = 8$ repetitions), the best configuration can instead obtain a service reliability of 12 h, with a communication service reliability above 99.99%.

VI. Conclusion

The requirements of IIoT are stricter than those of other IoT services. Therefore, LoRaWAN networks should be carefully configured in an industrial setting. In this article, we assessed the capability of the LoRaWAN technology in such scenarios by answering some key questions about how to properly configure the network.

The first outcome concerns the choice of an appropriate channel model, which is validated through empirical measurements for LoRa devices in industrial settings found in the literature. Results showed that, for a high-level performance analysis, the Spectrum interference model provided a good balance between accuracy and computational complexity. Secondly we showed that the increase of the GW density can improve all the metrics, and reduce the negative effect of duty cycle limitations. This, in turn, ameliorates the capability of transmitting DL messages, which brings benefits in terms of both ACK delay and reliability. Indeed, with a proper deployment and parameters configuration, and considering more lenient but reasonable application

requirements, we have shown that it is possible to achieve a delivery probability of over 99%, both in the UL-only and in the bi-directional communication. The frequency plan was a third point of investigation; using DR6 (i.e., employing a wider channel instead of three separate narrower channels) brings a slight degradation in the delay performance for the first transmission attempt, but improves it when more transmissions are needed, since the waiting time imposed by the duty cycle and the collision probability are both reduced. The combination of this frequency plan with the usage of Class C devices makes it possible to further reduce the delays for both UL and DL reception. Furthermore, we also demonstrated that, when a few GW are deployed, the usage of blind repetitions provides better performance than using confirmed traffic in terms of UL message delivery.

A LoRaWAN deployment can, therefore, meet the requirements of monitoring IIoT applications, if combined with a mindful choice of the devices and the network topology as well as a careful tuning of the parameters. Network designers must consider both the specific application requirements and the metrics of interest in order to devise a network deployment that satisfies the industrial needs without overprovisioning. However, if the envisaged applications dictate strict requirements, as presented in Section V-E, LoRaWAN still struggles to achieve such performance.

In the future, this work can be extended with the inclusion of Class B devices, which trade energy efficiency for latency of DL messages. This, combined with the introduction of longer data packets in the DL direction, would address those industrial applications that require periodic communication with the sensor nodes. Another interesting possibility of extension is the simulation of an outdoor industrial scenario, such as an industrial harbor, where the larger distances force nodes to use different SF, which is advantageous because of the quasi-orthogonality between SF, but at the same time, could require further analysis for the choice of optimal channel plan and GW positioning.

References

[1] E. Sisinni, A. Saifullah, S. Han, U. Jennehag, and M. Gidlund, "Industrial Internet of Things: Challenges, opportunities, and directions," *IEEE Trans. Ind. Informat.*, vol. 14, no. 11, pp. 4724–4734, Nov. 2018.

[2] E. Tanghe *et al.*, "The industrial indoor channel: Large-scale and temporal fading at 900, 2400, and 5200 MHz," *IEEE Trans. Wireless Commun.*, vol. 7, no. 7, pp. 2740–2751, Jul. 2008.

[3] D. Croce, M. Gucciardo, S. Mangione, G. Santaromita, and I. Tinnirello, "Impact of LoRa imperfect orthogonality: Analysis of link-level performance," *IEEE Commun. Lett.*, vol. 22, no. 4, pp. 796–799, Apr. 2018.

[4] Semtech Corporation, Camarillo, CA. USA, *SX1301 Datasheet*. Jun. 2014. [Online]. Available: https://www.semtech.com/products/wireless-rf/lora-gateways/sx1301#download-resources

[5] Semtech Corporation, Camarillo, CA. USA, *SX1272 datasheet*, Jun. 2015. [Online]. Available: https://www.semtech.com/products/wireless-rf/lora-transceivers/sx1272#download-resources

[6] "LoRaWAN 1.1 Specification," LoRa Alliance, Fremont, CA, USA, Oct. 2017. [Online]. Available: https://lora-alliance.org/resource-hub/lorawanr-specification-v11

[7] "ERC recommendation 70-03 - relating to the use of short range devices (SRD)," CEPT ECC, Copenhagen, Denmark, Tech. Rep., 2019.

[8] *Electromagnetic Compatibility and Radio Spectrum Matters (ERM)*, ETSI 300 220-1 v2. 4.1, 2012.

[9] D. Zucchetto and A. Zanella, "Uncoordinated access schemes for the IoT: Approaches, regulations, and performance," *IEEE Commun. Mag.*, vol. 55, no. 9, pp. 48–54, Sep. 2017.

[10] J. Ortin, M. Cesana, and A. Redondi, "Augmenting LoRaWAN performance with listen before talk," *IEEE Trans. Wireless Commun.*, vol. 18, no. 6, pp. 3113–3128, Jun. 2019.

[11] L. Leonardi, L. Lo Bello, F. Battaglia, and G. Patti, "Comparative assessment of the LoRaWAN medium access control protocols for IoT: Does listen before talk perform better than ALOHA?," *Electronics*, vol. 9, no. 4, Mar. 2020, Art. no. 553.

[12] R. Sanchez-Iborra and M.-D. Cano, "State of the art in LP-WAN solutions for industrial IoT services," *Sensors*, vol. 16, no. 5, May 2016, Art. no. 708.

[13] X. Li, D. Li, J. Wan, A. V. Vasilakos, C.-F. Lai, and S. Wang, "A review of industrial wireless networks in the context of industry 4.0," *Wireless Netw.*, vol. 23, no. 1, pp. 23–41, Nov. 2017.

[14] V. C. Gungor and G. P. Hancke, "Industrial wireless sensor networks: Challenges, design principles, and technical approaches," *IEEE Trans. Ind. Electron.*, vol. 56, no. 10, pp. 4258–4265, Oct. 2009.

[15] F. Bonavolontà, A. Tedesco, R. Schiano Lo Moriello, and A. Tufano, "Enabling wireless technologies for industry 4.0: State of the art," in *Proc. IEEE Int. Workshop Meas. Netw.*, 2017, pp. 1–5.

[16] A. Varghese and D. Tandur, "Wireless requirements and challenges in industry 4.0," in *Proc. Int. Conf. Contemporary Comput. Informat.*, 2014, pp. 634–638.

[17] J. P. Queralta, T. Gia, Z. Zou, H. Tenhunen, and T. Westerlund, "Comparative study of LPWAN technologies on unlicensed bands for M2M communication in the IoT: Beyond LoRa and LoRaWAN," *Procedia Comput. Sci.*, vol. 155, pp. 343–350, Aug. 2019.

[18] M. Capuzzo, D. Magrin, and A. Zanella, "Confirmed traffic in LoRaWAN: Pitfalls and countermeasures," in *Proc. 17th Annu. Mediterranean Ad Hoc Netw. Workshop*, Jun. 2018, pp. 1–7.

[19] A. I. Pop, U. Raza, P. Kulkarni, and M. Sooriyabandara, "Does bidirectional traffic do more harm than good in LoRaWAN based LPWA networks?," in *Proc. IEEE Glob. Commun. Conf.*, Dec. 2017, pp. 1–6.

[20] D. Magrin, M. Capuzzo, and A. Zanella, "A thorough study of LoRaWAN performance under different parameter settings," *IEEE Internet Things J.*, vol. 7, no. 1, pp. 116–127, Jan. 2020.

[21] T. R. Henderson, M. Lacage, G. F. Riley, C. Dowell, and J. Kopena, "Network simulations with the ns-3 simulator," in *Proc. SIGCOMM Demonstration*, Aug. 2008, p. 527.

[22] A. Hoeller, R. D. Souza, O. L. A. López, H. Alves, M. de Noronha Neto, and G. Brante, "Analysis and performance optimization of LoRa networks with time and antenna diversity," *IEEE Access*, vol. 6, pp. 32 820–32 829, 2018.

[23] F. Van den Abeele, J. Haxhibeqiri, I. Moerman, and J. Hoebeke, "Scalability analysis of large-scale LoRaWAN networks in ns-3," *IEEE Internet Things J.*, vol. 4, no. 6, pp. 2186–2198, Dec. 2017.

[24] J. Haxhibeqiri, A. Karaagac, F. V. den Abeele, W. Joseph, I. Moerman, and J. Hoebeke, "LoRa indoor coverage and performance in an industrial environment: Case study," in *Proc. 22nd IEEE Int. Conf. Emerg. Technol. Factory Automat.*, Sep. 2017, pp. 1–8.

[25] L. Tessaro, C. Raffaldi, M. Rossi, and D. Brunelli, "LoRa performance in short range industrial applications," in *Proc. Int. Symp. Power Electron., Elect. Drives, Automat. Motion*, 2018, pp. 1089–1094.

[26] W. Xu, J. Y. Kim, W. Huang, S. S. Kanhere, S. K. Jha, and W. Hu, "Measurement, characterization, and modeling of LoRa technology in multifloor buildings," *IEEE Internet Things J.*, vol. 7, no. 1, pp. 298–310, Jan. 2020.

[27] P. Neumann, J. Montavont, and T. Noel, "Indoor deployment of low-power wide area networks (LPWAN): A LoRaWAN case study," in *Proc. IEEE 12th Int. Conf. Wireless Mobile Comput., Netw. Commun.*, Oct. 2016, pp. 1–8.

[28] H. H. R. Sherazi, L. A. Grieco, M. A. Imran, and G. Boggia, "Energy-efficient LoRaWAN for industry 4.0 applications," *IEEE Trans. Ind. Informat.*, vol. 17, no. 2, pp. 891–902, Feb. 2021.

[29] M. Luvisotto, F. Tramarin, L. Vangelista, and S. Vitturi, "On the use of LoRaWAN for indoor industrial IoT applications," *Wireless Commun. Mobile Comput.*, vol. 2018, May 2018, Art. no. 3982646.

[30] M. Rizzi, P. Ferrari, A. Flammini, E. Sisinni, and M. Gidlund, "Using LoRa for industrial wireless networks," in *IEEE Proc. 13th Int. Workshop Factory Commun. Syst.*, May 2017, pp. 1–4.

[31] L. Leonardi, F. Battaglia, G. Patti, and L. L. Bello, "Industrial LoRa: A novel medium access strategy for LoRa in industry 4.0 applications," in *Proc. IECON Proc. 44th Annu. Conf. IEEE Ind. Electron. Soc.*, Oct. 2018, pp. 4141–4146.

[32] J. Navarro-Ortiz, S. Sendra, P. Ameigeiras, and J. M. Lopez-Soler, "Integration of LoRaWAN and 4G/5G for the Industrial Internet of Things," *IEEE Commun. Mag.*, vol. 56, no. 2, pp. 60–67, Feb. 2018.

[33] "Cellular system support for ultra-low complexity and low throughput Internet of Things (CIoT)," 3GPP, France, Tech. Rep. 45.820 V13.1.0, Nov. 2015.
[34] M. Cheffena, "Propagation channel characteristics of industrial wireless sensor networks [wireless corner]," *IEEE Antennas Propag. Mag.*, vol. 58, no. 1, pp. 66–73, Feb. 2016.
[35] Y. Ai, M. Cheffena, and Q. Li, "Radio frequency measurements and capacity analysis for industrial indoor environments," in *Proc. 9th Eur. Conf. Antennas Propag.*, 2015, pp. 1–5.
[36] M. Nakagami, "The m-distribution—A general formula of intensity distribution of rapid fading," in *Stat. Methods Radio Wave Propag.*, 1960, pp. 3–36.
[37] J. Ferrer-Coll, P. Ängskog, C. Elofsson, J. Chilo, and P. Stenumgaard, "Antenna cross correlation and Ricean K-factor measurements in indoor industrial environments at 433 and 868 MHz," *Wireless Pers. Commun.*, vol. 73, no. 3, pp. 587–593, May 2013.
[38] K. Blackard, T. Rappaport, and C. Bostian, "Measurements and models of radio frequency impulsive noise for indoor wireless communications," *IEEE J. Sel. Areas Commun.*, vol. 11, no. 7, pp. 991–1001, Sep. 1993.
[39] M. G. Sanchez, I. Cuinas, and A. V. Alejos, "Interference and impairments in radio communication systems due to industrial shot noise," in *Proc. IEEE Int. Symp. Ind. Electron.*, 2007, pp. 1849–1854.
[40] D. Magrin, M. Centenaro, and L. Vangelista, "Performance evaluation of LoRa networks in a smart city scenario," in *Proc. IEEE Int. Conf. Commun.*, 2017, pp. 1–7.
[41] ETSI, "Technical characteristics for Low Power Wide Area Networks Chirp Spread Spectrum (LPWAN-CSS) operating in the UHF spectrum below 1 GHz (TR 103 526)," Apr. 2018. [Online]. Available: https://www.etsi.org/deliver/etsi_tr/103500_103599/103526/01.01.01_60/tr_103526v010101p.pdf
[42] "Application note: LoRa modulation crystal oscillator guidance," Semtech, Camarillo, CA. USA, Tech. Rep. AN1200.14 Rev. 2, 2017.
[43] "RF performance tests of LoRa gateways without an external network server," RedwoodComm, Goyang, South Korea, Appl. Note RWC5020A PC Appl. Softw. RAN1940001-rev2, 2019.
[44] D. Croce, M. Gucciardo, S. Mangione, G. Santaromita, and I. Tinnirello, "LoRa technology demystified: From link behavior to cell-level performance," *IEEE Trans. Wireless Commun.*, vol. 19, no. 2, pp. 822–834, 2020.
[45] "Technical specification group services and system aspects; service requirements for cyber-physical control applications in vertical domains; Stage 1," 3GPP, France, Tech. Rep. 22.104 V.17.4.0, Sep. 2020.

Davide Magrin (Member, IEEE) received the M.Sc. in telecommunications engineering in 2014, from the University of Padova, Padova, Italy, where he is currently working toward the Ph.D. degree with the Department of Information Engineering, under the supervision of Prof. M. Zorzi. During his Ph.D. he collaborated with research groups with the University of Washington, Seattle, WA, USA, and University of Naples, Naples, Italy.

His research interests include development and validation of simulation models for Internet of Things technologies, modeling of LoRaWAN and 802.11 networks, the evaluation of such networks in various application scenarios, and the design of novel solutions for network management and optimization.

Martina Capuzzo (Student Member, IEEE) received the bachelor's degree in information engineering and the master's degree (cum laude) in telecommunications engineering from the University of Padova, Padova, Italy, in 2015 and 2018, respectively. She is currently working toward the Ph.D. degree in information engineering with the Department of Information Engineering with the University of Padova. She collaborated with the Simula Research Center and Telenor Group, Oslo (NO), and with the IDLab research group, University of Antwerp (BE), Antwerp, Belgium.

Her research interests include performance analysis of Internet of Things networks, with a particular focus on LoRaWAN, its evaluation in different application scenarios, and its combination with battery-less devices and harvesting solutions.

Andrea Zanella (Senior Member, IEEE) received the Laurea degree in computer engineering and the Ph.D. degree in electronic and telecommunications engineering from the University of Padova, Padova, Italy, in 1998 and 2001.

He is a Full Professor with the Department of Information Engineering (DEI), University of Padova, Padova, Italy. During 2000, he was a Visiting Scholar with the University of California, Los Angeles, CA, USA, within Prof. Mario Gerla's research team. He has authored or coauthored more than 190 papers. His research interests include protocol design, optimization, and performance evaluation of wired and wireless networks.

He has been serving on the editorial board of several top journals, such as IEEE INTERNET OF THINGS JOURNAL, IEEE COMMUNICATIONS SURVEYS AND TUTORIALS, and IEEE TRANSACTIONS ON COGNITIVE COMMUNICATIONS AND NETWORKING.

Lorenzo Vangelista (Senior Member, IEEE) received the Laurea and Ph.D. degrees in electrical and telecommunication engineering from the University of Padova, Padova, Italy, in 1992 and 1995, respectively.

He joined the Transmission and Optical Technology Department, CSELT, Torino, Italy, in 1995. From December 1996 to January 2002, he was with Telit Mobile Terminals, Trieste, Italy, and then, until May 2003, he was with Microcell A/S, Copenaghen, Denmark. In July 2006, he joined the Worldwide Organization of Infineon Technologies as Program Manager. Since October 2006, he has been an Associate Professor of Telecommunications with the Department of Information Engineering, Padova University. His research interests include signal theory, multicarrier modulation techniques, cellular networks and Internet of Things connectivity with special focus on low power wide area networks.

Michele Zorzi (Fellow, IEEE) received the Laurea and Ph.D. degrees in electrical engineering from the University of Padova, Italy, in 1990 and 1994, respectively.

After holding several academic positions in both Italy and USA, since November 2003, he has been a Professor with the University of Padova. His current research interests include performance evaluation in mobile communications systems, WSN and the Internet of Things, cognitive communications and networking, 5G mmWave cellular systems, vehicular networks, and underwater communications and networks.

Dr. Zorzi has served the IEEE Communications Society as a Member-at-Large of the Board of Governors, from 2009 to 2011, as the Director of Education, in 2014 and 2015, and as the Director of Journals, since 2020. He was the recipient of several awards from the IEEE Communications Society, including the Best Tutorial Paper Award, in 2008 and 2019, the Education Award, in 2016, the Joseph LoCicero Award for Exemplary Service to Publications, in 2020, and the Stephen O. Rice Best Paper Award, in 2018. He was three-time Editor-in-Chief for IEEE periodicals.